Design and experimental validation of the high-speed counter-rotating thresher for pomegranate aril extraction

Peifeng Ma[1,2], Aibin Zhu[1,2*], Jing Zhang[3*], Han Mao[3], Chunli Zheng[4], Jinping Huang[3], Jing Wang[2], Bingsheng Bao[2], Chong Gao[3], Dangchao Li[3]

(1. *Institute of Robotics & Intelligent Systems, Xi'an Jiaotong University, Xi'an 710049, China*;
2. *Shaanxi Key Laboratory of Intelligent Robots, Xi'an 710049, China*;
3. *Key Laboratory of Education Ministry for Modern Design and Rotor-Bearing System, Xi'an 710049, China*;
4. *School of Energy and Power Engineering, Xi'an Jiaotong University, Xi'an 710049, China*)

Abstract: This study presents the design and experimental validation of a high-speed, drum-type pomegranate thresher driven by an innovative single-drive, multi-shaft transmission system. This design integrates crushing, feeding, and threshing into a compact unit, significantly reducing mechanical complexity and energy consumption. Finite element analysis verified the structural integrity of key components under operational loads. Systematic experiments identified an optimal speed of 220 r/min, achieving a threshing efficiency of 28.6 pieces/min, a peel removal rate of 88.3%, and an aril damage rate of 12.6%. The incorporation of a pre-crushing mechanism enhanced overall efficiency by 30.6%, a performance gain analyzed as a trade-off against a manageable increase in aril damage. The device demonstrated robust adaptability, processing fresh and stored pomegranates at rates of 33.9 and 27.9 pieces/min, respectively, while revealing critical correlations between pomegranate physical properties and threshing outcomes. This work provides an efficient and scalable solution for industrial pomegranate processing and establishes a foundation for future intelligent control systems.

Keywords: pomegranate, high-speed thresher, drum-type thresher, strength analysis
DOI: 10.25165/j.ijabe.20261901.10057

Citation: Ma P F, Zhu A B, Zhang J, Mao H, Zheng C L, Huang J P, et al. Design and experimental validation of the high-speed counter-rotating thresher for pomegranate aril extraction. Int J Agric & Biol Eng, 2026; 19(1): 302–308.

1 Introduction

Pomegranate is a highly nutritious fruit, rich in vitamins, polyphenols, and trace elements, which have garnered increasing attention due to their health benefits[1-3]. As market demand for pomegranates continues to rise, the fruit's processing has become increasingly important[4-6]. However, industrial pomegranate processing faces significant challenges, particularly in the dehulling process, which remains inefficient and labor-intensive. Manual threshing not only incurs high labor costs but also leads to inconsistent product quality[7,8].

Current mechanical threshing technologies for pomegranates are primarily classified into two types: impact-type and drum-type devices[9-12]. Impact-type threshers typically require the fruit to be cut and manually positioned before threshing via oscillating or striking mechanisms. These devices, though effective, suffer from low throughput and high dependency on manual labor[13-16]. Drum-type threshers, which utilize rotating drums and beating rods, are more automated but often result in high energy consumption and aril damage due to mechanical impacts and inefficient transmission systems[17-19]. Additionally, many drum-type devices rely on complex multi-motor configurations, which increase both structural complexity and maintenance requirements[20-23].

To address these challenges, this study introduces a new type of drum-type high-speed pomegranate threshing device. Beyond structural optimization, this study addresses a key scientific gap: the lack of a systematic understanding of the intrinsic correlation between pomegranate physical properties and threshing performance. To overcome these engineering bottlenecks and investigate their underlying mechanisms, this work is built upon three complementary pillars:

1) An innovative single-drive multi-axis transmission system has been proposed to eliminate complex multi-motor configurations, thereby directly reducing mechanical complexity, energy consumption, and costs.

2) Adopting rigorous finite element analysis (FEA) to verify the structural strength and reliability of key components under high-speed operating loads, ensuring their robustness and design adequacy.

3) A comprehensive experimental activity was conducted, including speed optimization and variety adaptability testing, not only to find the optimal working parameters, but also to quantitatively analyze how fruit status and equipment parameters affect threshing efficiency and aril integrity.

Through a combination of mechanism-driven design, virtual

Received date: 2025-07-29 **Accepted date:** 2025-12-02
Biographies: **Peifeng Ma**, PhD candidate, research interest: agricultural automation, Email: 2690018763@qq.com; **Han Mao**, PhD candidate, research interest: mechanical transmission systems, Email: maohan0325@126.com; **Chunli Zheng**, PhD, research interest: energy efficiency optimization, Email: clzheng@mail.xjtu.edu.cn; **Jinping Huang**, PhD candidate, research interest: robot control systems, Email: 1140948791@qq.com; **Jing Wang**, PhD, research interest: intelligent algorithms, Email: wangpele@gmail.com; **Bingsheng Bao**, PhD candidate, research interest: robotic perception, Email: 1104634004@qq.com; **Chong Gao**, MS, research interest: computer vision, Email: gaochong@xjtu.edu.cn; **Dangchao Li**, BS, research interest: mechatronic systems design, Email: ldc.061@xjtu.edu.cn.

***Corresponding author: Aibin Zhu**, Professor, research interest: intelligent robotics. Institute of Robotics & Intelligent Systems, Xi'an Jiaotong University, Xi'an 710049, China. Tel: +86-18629000528, Email: abzhu@mail.xjtu.edu.cn; **Jing Zhang**, PhD candidate, research interest: robotics design. Key Laboratory of Education Ministry for Modern Design and Rotor-Bearing System, Xi'an 710049, China. Tel: +86-18093640182, Email: jzhang.phd@stu.xjtu.edu.cn.

strength validation, and empirical performance decision analysis, this study aims to provide an efficient, reliable, and scientific solution for the pomegranate processing industry, as well as a scalable model for other fruit processing industries. The following section provides a detailed introduction to the design, analysis, and experimental verification of the proposed equipment.

2 Structure and principle

2.1 Overall structure

The drum-type high-speed pomegranate threshing device integrates the key processes of crushing, feeding, and threshing into a compact and efficient system, all powered by a single gear motor. The system employs a multi-shaft chain and gear transmission mechanism that drives all key components: counter-rotating, rubber-coated crushing rollers, a screw-type feeding mechanism, and a cylindrical threshing drum equipped with helically arranged threshing rods. These components are mounted on a shared frame to ensure structural stability and coordinated operation.

The motor delivers power to the system through a chain drive, which transmits torque to the main spindle, the spiral feeding mechanism, and the rotating threshing drum. To facilitate counter-rotation between the rollers and the sieve drum, appropriately designed gear pairs are used. These gear pairs allow the rollers and drum to rotate in opposite directions, thereby increasing the relative impact speed between components, which enhances threshing efficiency while reducing aril breakage.

The system is designed for optimal synchronization of all subsystems. Speed regulation ensures that each component operates in harmony, ensuring smooth transitions between processes. By combining these functions into a single-drive, multi-shaft transmission system, this design reduces mechanical complexity and improves energy efficiency. This innovative approach simplifies the structure and minimizes the need for additional power sources, leading to lower energy consumption and more efficient operation. The overall system layout is shown in Figure 1, where the key components and their integration can be observed.

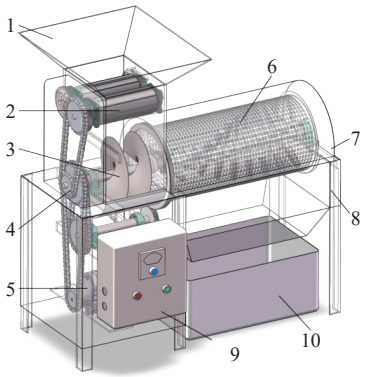

1. Feeding port 2. Dual-roller squeezing and crushing device 3. Spiral feeding mechanism 4. Single-drive multi-shaft transmission system 5. Gear motor 6. Counter-rotating sieve-based threshing mechanism 7. Discharge port 8. Frame 9. Speed control cabinet 10. Aril collection box

Figure 1 Overall structure of the drum-type high-speed pomegranate threshing equipment

2.2 Working principle

The drum-type high-speed pomegranate threshing device integrates crushing, feeding, and threshing functions into a compact system powered by a single gear motor. A multi-shaft chain and gear transmission system drives key components: counter-rotating rubber-coated rollers, a screw-type feeding mechanism, and a cylindrical threshing drum with helically arranged threshing rods. The motor transmits power to all components via a chain drive, ensuring synchronized operation. Gear pairs enable counter-rotation between the drum and rollers, optimizing impact speed and reducing aril breakage. This modular design minimizes mechanical complexity, enhances energy efficiency, and reduces the need for additional motors.

3 Key component design and analysis

3.1 Design of the single-drive multi-shaft transmission system

The single-drive multi-axis transmission system distributes power from a 4 kW gear motor (output speed: 150-450 r/min) to the screw feeder, dual-roll crusher, and counter-rotating threshing cylinder. Chain drive was employed for effective power transmission between parallel shafts. As shown in Figure 2, the motor drives the main shaft via chain, which subsequently powers both the crushing rolls and threshing drum. Counter-rotation between components such as the rolls and screen cylinder is achieved through integrated gear pairs.

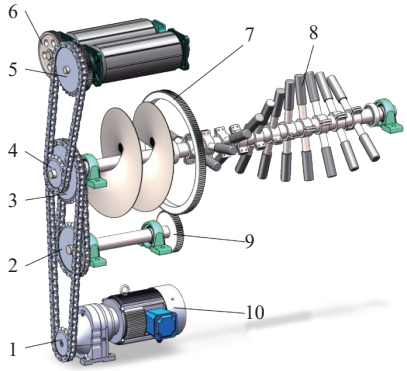

1. Motor output sprocket 2. Sieve drive sprocket 3. Main shaft drive sprocket 4. Small sprocket on main shaft 5. Crushing roller sprocket 6. Gear set for rollers 7. Sieve gear ring 8. Threshing rods 9. Sieve gear 10. Gear motor

Figure 2 Design of single-drive multi-shaft combined transmission system

To meet the design goal of processing 1800 pomegranates per hour, a transmission scheme featuring a 2:1 reduction ratio was implemented. Based on GB/T1243 standards, 16A-type roller chains were selected. Detailed calculations were performed to determine the optimal sprocket tooth numbers, chain pitch, wrap angles, and center distances. The final transmission parameters—including gear ratios, shaft spacing, chain lengths, and link counts—are summarized in Table 1, confirming that all design conditions satisfy mechanical and operational requirements.

Table 1 Reduction ratios between shafts of multi-shaft combined transmission system

Transmission pair	Speed ratio	Center distance/mm	Chain links	Chain length/m
Motor output shaft–main shaft	2.0	757	84	2.130
Main shaft–sieve drive shaft	1.5	346	50	1.270
Main shaft–roller drive shaft	1.5	498	62	1.575

3.2 Design of the dual-roller squeezing and crushing mechanism

The crushing unit uses two rubber-coated rollers with ridged surfaces rotating in opposite directions via gear coupling to gently pre-break the pomegranates. When the fruit enters the roller gap

along the bisector of the roller axes, it is clamped and entrained into the narrowing space. As shown in Figure 3, the fruit experiences symmetrical normal and frictional forces, along with gravity. The crushing performance is influenced by roller radius, spacing, and surface characteristics[24,25].

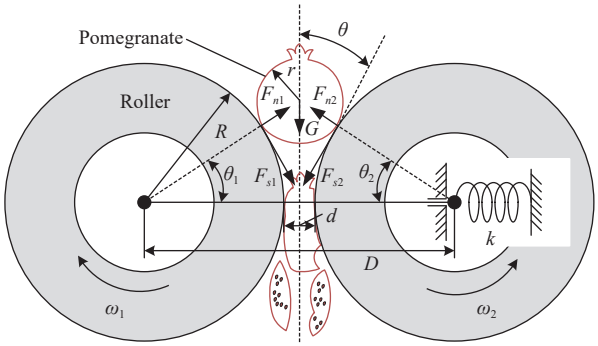

Note: F_{n1}, F_{n2}: normal forces F_{s1}, F_{s2}: frictional forces w_1, w_2: angular velocities R: roller radius d: gap distance D: the center distance

Figure 3 Force analysis of pomegranate entering roller extrusion work area

The condition for successful clamping and crushing can be expressed as:

$$\theta < \arcsin\left(\frac{G}{2F_n\cos\varphi}\right) - \varphi \quad (1)$$

where, θ is the angle between the line connecting roller centers and the direction of the applied normal force, °; φ is the friction angle between the squeezing roller and the surface of the pomegranate, °.

A simplified force analysis shows that the relative magnitude of normal and frictional forces is governed by the roller radius and center distance. When the roller radius is too small or the spacing too wide, the pomegranate may slip through the rollers without sufficient compression. Conversely, excessive pressure angles caused by large spacing or undersized rollers may lead to inefficient crushing or damage. Therefore, appropriate sizing of roller diameter and gap is essential to ensure reliable crushing and high threshing efficiency.

3.3 Design of the counter-rotating sieve-based threshing unit

As shown in Figure 4, the rotary screen cylinder adopts a two-stage design: the front section is a spiral feeding blade, and the rear section is a perforated screen with a hole diameter of 15 mm, optimized for Xinjiang Piaman pomegranate, with an average aril diameter of 10 mm. The drum is driven by a gear ring connected to the gear shaft and rotates opposite to the motor output shaft. This reverse rotation configuration increases the relative speed between the rod and the drum. At the same time, the spindle of the threshing rod equipped with a spiral arrangement rotates in the same direction as the motor. The shape, geometry and spatial arrangement of the threshing rod are key parameters that directly determine the threshing efficiency and aril damage rate. The selection of these specific parameters is to achieve high peel removal rate while actively managing aril damage rate.

1) Shape and geometry: The threshing rod is designed as a cylindrical shape and coated with a soft rubber layer. The choice of this shape factor is to minimize stress concentration when colliding with arils, thereby reducing puncture and crushing damage compared to sharp edges or rigid profiles. The threshing rod provides sufficient stiffness for force transmission while maintaining a flexible contact surface.

2) Arrangement rule: The rods are arranged in a double helix along the main axis, and the two main functions of this helix arrangement are axial conveying and uniform threshing and covering. The spiral angle produces a continuous spiral conveying effect, ensuring that the crushed pomegranate material is pushed axially from the feed end to the discharge port. This controls the residence time of the material in the threshing cylinder. The double helix structure ensures that the rod scans the entire internal volume of the sieve cylinder, preventing local dead zones and promoting a more uniform and thorough separation of the aril and fruit peel.

3) Interaction with the sieve cylinder: The reverse rotational motion between the main shaft and the sieve cylinder creates a high shear, rolling compression zone in the gap between them. The rod mainly connects larger fruit peel fragments, applying bending and shear stress to release the arils. The released arils are smaller than the sieve aperture and are quickly discharged through the sieve, minimizing their repeated impact and thus reducing secondary damage.

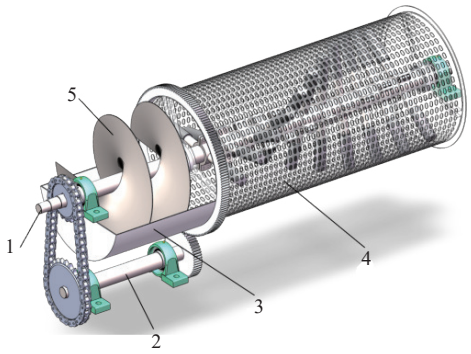

1. Threshing spindle 2. Sieve gear shaft 3. Feed barrel 4. Sieve drum 5. Spiral feeding blades

Figure 4 Mechanical structure of opposite rotary screen thresh device

4 Strength analysis of key components

During operation, pomegranates are first crushed by the dual-roller mechanism and then conveyed by the spiral blade on the main spindle into the counter-rotating sieve for threshing. The dual-roller crushing unit, main spindle, spiral blade, and threshing rods are therefore key components of the system. To validate their mechanical robustness, finite element analysis (FEA) was conducted using the Simulation module in SolidWorks.

4.1 Strength analysis of the crushing roller

The dual-roller squeezing device consists of a central drive shaft and an outer rubber-coated roller, as shown in Figure 5a. The drive shaft is made of stainless steel and is subjected to torsional loading during operation. To evaluate its mechanical performance under extreme conditions, the FEA was performed. In the simulation, the end of the shaft was fixed, and a maximum torque of 414.66 N·m, derived from the motor output and chain transmission ratio, was applied at the shaft center. The FEA mesh model is shown in Figure 5b.

Simulation results under torsional load reveal the stress distribution and deformation characteristics shown in Figure 5c and Figure 5d, respectively. The maximum von Mises stress reached 135 MPa, which is well below the material's yield strength, indicating structural safety. The maximum displacement was 7.75 mm, primarily concentrated in the outer rubber layer. This localized deformation does not interfere with normal roller functionality, confirming the adequacy of the design for operational reliability.

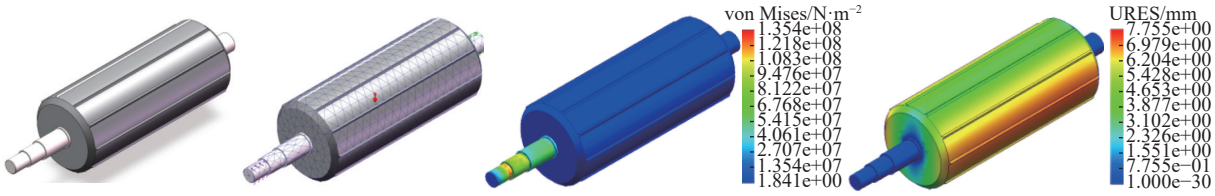

a. 3D model of the roller b. Mesh and applied torque c. von Mises stress distribution d. Displacement distribution

Figure 5 Strength analysis of single extrusion roller

4.2 Strength analysis of the main spindle and assembly

After the pomegranates are crushed, they are conveyed into the cylindrical sieve drum by the main spindle, which drives the spiral feeding blades through rotational motion. The spindle and its associated components are shown in Figure 6a. Except for the threshing rods, which are coated with soft rubber, all other parts are made of stainless steel. The spindle is subjected to multiple loads during operation, including a spindle drive torque of 170 N·m, an axial resistance force of 200 N from the spiral blades, and a combined reaction force of 100 N generated by the impact of the threshing rods on the fruit. These loads were applied to the finite element model, and meshing was performed as shown in Figure 6b.

a. 3D model of the spindle with spiral and rods b. Mesh and loading scheme c. von Mises stress distribution d. Displacement field

Figure 6 Strength analysis of spindle and its assembly parts

The simulation results are presented in Figure 6c and Figure 6d, showing the stress distribution and deformation patterns of the spindle assembly. The maximum von Mises stress, located near the spindle's input section, is 24.0 MPa—well below the material's yield strength—indicating sufficient structural strength for safe operation. However, due to the use of rubber on the threshing rods, the maximum deformation reaches 24.4 mm at the rod tips. This suggests that the rubber layer is prone to wear and fatigue over time. To ensure long-term stability and threshing performance, periodic replacement of the rubber coating is recommended during routine equipment maintenance.

5 Prototype testing and results

5.1 Evaluation metrics

To evaluate the threshing performance of the proposed device, three key metrics were adopted: threshing efficiency, peel removal rate, and aril damage rate. To determine the peel removal rate and aril damage rate, it is necessary to sample the arils after experimental cleaning three times, separate damaged arils and residual peels, measure the sample mass using a grammage electronic scale (0-500 g), and calculate the indicators. The schematic diagram of sampling separation and weighing is shown in Figure 7.

Threshing efficiency, reflecting the processing capacity per unit time of the equipment, is calculated by:

$$q = \frac{n}{t} \tag{2}$$

where, q is the threshing efficiency, pieces/min; n is the total number of pomegranates processed, pieces; and t is the total processing time, min.

Peel removal rate, characterizing the thoroughness of separation, is given by:

$$\mu = 1 - \frac{m_r}{m_g} \times 100\% \tag{3}$$

where, μ is the peel removal rate; m_r is the mass of residual peel, g; and m_g is the total mass of sampled arils, g.

Aril damage rate, evaluating threshing-induced damage, is calculated as:

$$v = \frac{m_i}{m_g} \times 100\% \tag{4}$$

where, v is the aril damage rate; m_i is the mass of damaged arils, g; and m_g is the total mass of sampled arils, g.

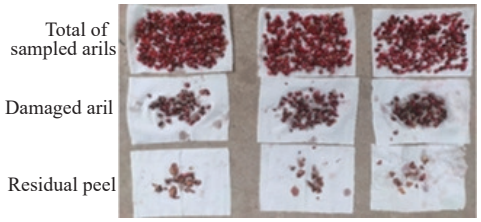

a. Sampling separation

b. Weighing

Figure 7 Schematic diagram of sampling separation and weighing

5.2 Speed optimization experiment

Based on the proposed mechanical structure, motor specifications, and selected materials, a functional prototype of the high-speed pomegranate threshing device was developed. As shown in Figure 8a, the system features a compact layout that integrates crushing, feeding, and threshing modules.

For the experiment, Xinjiang Piaman pomegranates with diameters of 5-7 cm and average mass of 350-450 g were selected. Preliminary tests verified effective threshing results as seen in

Figure 8b.

Prototype tests were conducted at six gear motor speed levels (200-250 r/min), testing 50 pomegranates per level. Performance metrics of the drum-type equipment were quantified to characterize speed-dependent effects on threshing performance, as listed in Table 2.

a. Physical prototype b. Ariled pomegranate sample

Figure 8 Pomegranate thresher prototype and its threshing effect

Table 2 Test data of pomegranate thresher

Level	Motor speed/ r·min^{-1}	Threshing time/min	Total mass of sampled arils/g	Residual peel mass/g	Damaged aril mass/g
1	200	2.06	87.3	9.2	11.6
2	210	1.92	89.3	7.8	11.3
3	220	1.75	78.4	9.2	9.8
4	230	1.68	66.0	8.0	8.9
5	240	1.65	66.6	10.0	12.2
6	250	1.59	59.7	9.7	11.5

Based on these measurements, the relationships between motor speed and the three evaluation metrics were plotted and analyzed, as shown in Figure 9. The data show that both threshing efficiency and peel removal rate exhibit a positive linear relationship with operating speed. Their empirical models are expressed as:

$$\begin{aligned} y_1 &= 0.1424x - 3.6458 \\ y_2 &= -0.0014x + 1.1831 \end{aligned} \quad (5)$$

where, y_1 is the threshing efficiency, pieces/min; y_2 is the peel removal rate; and x is the motor speed, r/min.

Through the above experiment, the relationship between motor speed and performance indicators can be directly attributed to the dynamics of the threshing rod. The linear increase in threshing efficiency with speed is the result of the increase in impact frequency and shear rate generated by the helical arrangement of rods. As the spindle rotation speed increases, the number of times the rod passes through and stirs the material per unit time increases, thereby accelerating the separation process.

The nonlinear trend of rod damage rate is a key result of the interaction between rod materials. At lower speeds (such as 200 r/min), the impact energy may not be sufficient for cleaning and separation, causing the arils to be repeatedly rubbed and squeezed by the rod and peel fragments, resulting in cumulative damage. At the optimal speed (220 r/min), the impact and shear forces are sufficient to cleanly separate arils with minimal contact repetition, thereby minimizing damage. At higher speeds (such as 250 r/min), the kinetic energy of the rod becomes too high. The impact force during collision may exceed the breaking stress of arils, leading to a sharp increase in fracture. This indicates that the rubber coating on the rod can alleviate but not completely eliminate damage caused by excessive energy input.

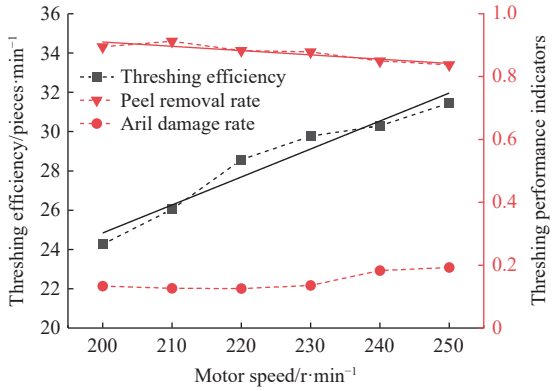

Figure 9 Relationship curve between pomegranate running speed and related test indices

When the output speed of gear motor reaches the optimal equilibrium point at 220 r/min, its threshing efficiency is 28.6 pieces/min, an increase of 17.7% compared to the lowest speed. At the same time, the peel removal rate is 88.3% and the aril damage rate is 12.6%, which fully meet the industry standard requirements. The determination of this optimal parameter provides benchmark conditions for subsequent experiments.

5.3 Efficiency verification of crushing device

To quantify the synergistic effect of the roller squeezing and crushing device on threshing performance, two groups were compared: a control group without this device and an experimental group with the complete equipment configuration as shown in Figure 10. All experiments were conducted at the optimal speed of 220 r/min using 50 Xinjiang Piaman pomegranates per group, repeated in triplicate. Pomegranates were manually fed into the threshing machines, with processing times recorded and the procedure video-recorded.

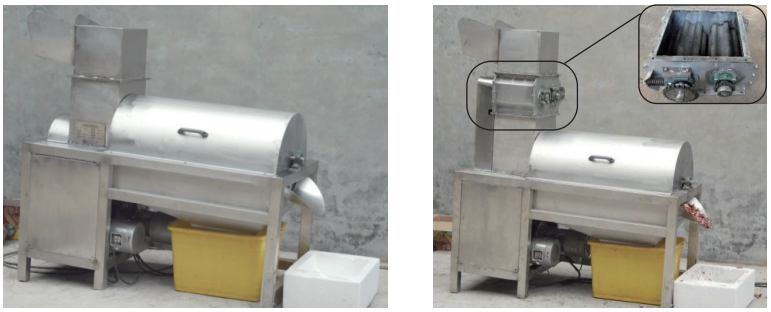

a. Control group: Equipment 1 b. Experimental group: Equipment 2

Figure 10 Control group and experimental group device

Experimental results in Table 3 demonstrate that the pre-crushing mechanism significantly improves both threshing efficiency and peel removal rate. However, this enhancement comes at the cost of increased aril damage, which rose from 12.8% to 17.0%. This trade-off arises from two primary factors:

1) Aril pre-weakening: The compressive and shear forces applied by counter-rotating rollers to fracture the hard peel are essential but may induce microcracks or residual stresses in arils within the compression zone. Such pre-weakened arils are more susceptible to subsequent damage during intensive threshing in the rotary drum. In contrast, the control group, lacking this pre-compression step, processes fruits with pre-broken peels but without aril pre-weakening.

2) Roller wear: As discussed in the strength analysis (Section 4.2), roller rubber coatings undergo progressive wear. Worn rollers lose uniform flexibility, creating localized high-pressure points rather than distributing gentle compressive forces. This uneven loading exacerbates aril damage during pre-crushing.

Table 3 Comparison of threshing performance indicators with and without crushing devices

Index	Control group	Experimental group	Increase amplitude
Threshing efficiency/pieces·min^{-1}	24.2	31.6	30.6%
Peel removal rate/%	82.4	89.7	7.3%
Aril damage rate/%	12.8	17.0	4.2%

Despite the elevated damage rate, threshing efficiency and peel removal rate increased by 30.6% and 7.3%, respectively, confirming the overall effectiveness of the 'pre-crushing differential threshing' mechanism. The substantial gains in throughput and separation quality justify this controlled damage increase. Future research will focus on optimizing extrusion parameters—including roller gap, speed, and rubber hardness—and implementing adaptive control systems to precisely regulate pre-crushing intensity, thereby minimizing damage while preserving efficiency gains.

5.4 Variety adaptability experiment

To compare device threshing performance across pomegranate conditions and against manual methods, two experimental groups were established alongside a concurrent manual control. Group A comprised pomegranates stored for six months, exhibiting severe dehydration (peel thickness: 2.8±0.3 mm); Group B comprised freshly harvested pomegranates (<24 h post-harvest) with high turgor (peel thickness: 4.2±0.5 mm) (Figure 11). Machine threshing trials were conducted at the optimal speed of 220 r/min using 50 fruits per group, repeated in triplicate. The manual control group utilized identical fruit batches processed by skilled workers, with the entire process timed via stopwatch and video-recorded.

As listed in Table 4, threshing efficiency for fresh pomegranates (33.9 pieces/min) significantly exceeds that for stored pomegranates (27.9 pieces/min). This disparity stems from post-storage moisture loss, which increases peel fracture toughness and requires greater rupture forces. Simultaneously, dehydration-induced aril brittleness is not matched by proportional weakening of aril-septum attachments, further elevating separation difficulty.

Accordingly, the aril damage rate for stored pomegranates (15.3%) exceeds that for fresh fruit (12.6%). Stored arils exhibit increased brittleness and reduced impact tolerance. To overcome toughened peel and persistent adhesion, the equipment must prolong action time or concentrate force at equivalent speeds, heightening the risk of excessive mechanical loading. Additionally, intrinsic brittleness of stored arils contributes to this elevated damage susceptibility.

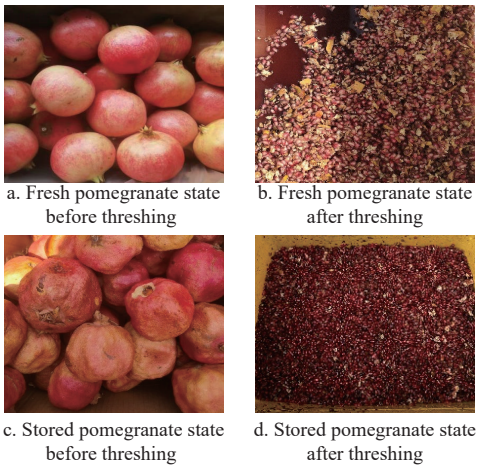

a. Fresh pomegranate state before threshing b. Fresh pomegranate state after threshing

c. Stored pomegranate state before threshing d. Stored pomegranate state after threshing

Figure 11 Status of pomegranate varieties before and after threshing

Table 4 Comparison of threshing performance indicators with and without crushing devices

Index	Experimental group A	Experimental group B	Artificial control group
Threshing efficiency/pieces·min^{-1}	27.9	33.9	3.2
Increase/%	762.5	959.4	-
Peel removal rate/%	82.1	88.3	91.7
Aril damage rate/%	15.3	12.6	8.4

Collectively, these results preliminarily establish an intrinsic relationship between pomegranate physical properties and threshing performance:

Peel thickness: a critical factor influencing threshing efficiency and peel removal rate. Freshly harvested pomegranates with thick peels fracture readily during compression and initial impact, thereby facilitating subsequent threshing operations. Conversely, pomegranates with thin peels demand significantly greater energy and time inputs, often yielding incomplete separation with peel fragments contaminating the arils.

Aril adhesion: directly influences aril damage rates. Elevated adhesion necessitates greater separation forces; however, if inadequately controlled, these forces may exceed the compressive/shear strength thresholds of the arils, resulting in mechanical damage. The rotary kneading threshing mechanism employed in this equipment generates sustained shear forces that, compared with pure impact-type methods, more effectively overcome adhesion while concurrently reducing peak impact forces.

The 'pre-crushing differential threshing' mechanism of this device is specifically engineered to accommodate these characteristics. The reverse-rotating drum gently pre-cracks the fruit through compressive stress, effectively reducing the peel toughness barrier. Subsequently, the reverse-rotating threshing drum generates sustained shear forces that, being more effective and controllable than pure impact, successfully overcome aril adhesion while optimizing the efficiency-damage trade-off.

At the optimal speed of 220 r/min, fresh pomegranate threshing efficiency reached 33.9 pieces/min in the variety adaptability experiment, exceeding the 31.6 pieces/min recorded at the same speed in the crushing device comparison (Section 5.3). This discrepancy is attributed primarily to inherent batch-to-batch variations in physical properties (size and peel toughness) between

the samples used in these independent studies—a common phenomenon in agricultural product processing.

6 Conclusions

This study designed and validated a drum-type high-speed pomegranate threshing device, providing a comprehensive solution to the bottleneck of low efficiency and high damage in existing mechanical processing methods. The core innovation lies in the single-drive multi-axis transmission system, which integrates crushing, feeding, and threshing functions under one power source, significantly reducing mechanical complexity and energy consumption. The structural reliability of key components, including the crushing roller and spindle assembly, was rigorously verified through finite element analysis, confirming that all maximum stresses remained within a safe range under operating loads. This virtual verification ensures the robustness of the device during high-speed operation.

A quantitative relationship between operating parameters and threshing performance was established through system experiments. The speed optimization experiment determined 220 r/min as the optimal working point, achieving a balance between a threshing efficiency of 28.6 pieces/min, a peel removal rate of 88.3%, and a aril damage rate of 12.6%. The comparative experiment of the crushing device ultimately proved the key role of the pre-crushing mechanism, which increased the overall threshing efficiency by 30.6% and the peel removal rate by 7.3%. In addition, the study conducted an in-depth analysis of the intrinsic correlation between the toughness of pomegranate peel and the adhesion of aril with threshing results. This mechanical understanding explains the performance difference between fresh pomegranates and stored pomegranates, with the equipment achieving processing efficiencies of 33.9 pieces/min and 27.9 pieces/min for fresh and stored pomegranates, respectively.

This device has excellent engineering applicability and scalability. Its modular design allows for adaptation to different pomegranate varieties. Future work will focus on developing intelligent adaptive control systems. The system will use real-time sensor signals to drive motor torque and machine vibration characteristics as inputs. Then, the control algorithm will dynamically adjust key parameters such as roller clearance and feed rate in real time. This closed-loop strategy aims to further improve the balance between efficiency and integrity, paving the way for the next generation of intelligent fruit processing equipment. The technical solutions and design methods proposed in this article have significant value for the pomegranate industry and provide valuable references for the development of other fruit processing machinery.

Acknowledgements

This work was supported by the National Natural Science Foundation of China (Grant No. 52575073), and in part by the National Key Research and Development Program of China (Grant No. 2023YFC3604903), and in part by the Shaanxi Provincial Key R&D Program (Grant Nos. 2025SF-YBXM-466, 2025CY-YBXM-098, 2025CY-YBXM-349, 2024PT-15, 2024NC-YBXM-192, 2024SF-ZDCYL-04-12, 2024SF-YBXM-449, and 2024GX-YBXM-287).

[References]

[1] Siddiqui S A, Singh S, Nayik G A. Bioactive compounds from pomegranate peels-Biological properties, structure–function relationships, health benefits and food applications–A comprehensive review. Journal of Functional Foods, 2024; 116: 106132.

[2] Kandylis P, Kokkinomagoulos E. Food applications and potential health benefits of pomegranate and its derivatives. Foods, 2020; 9(2): 122.

[3] Yu X H, Shen C Y. Current status and promotion prospects of the pomegranate industry in China. Rural Science and Technology, 2019; 9(22): 36–37. (in Chinese)

[4] Li F, Qin C H, Ding Z Q. Research progress on pomegranate peel in traditional Chinese and western medicine. Guide China Med, 2022; 20(25): 69–71. (in Chinese)

[5] Tian H L, Qu Y C, Zhou Q H, Huang R T, Yin Z G, Fan C Y, et al. Research progress on development and application of homologous pomegranate for medicine and food. Cereal & Food Industry, 2022; 29(3): 27–31. (in Chinese)

[6] Xu Y F, Zhao S J, Fei P, Xiang J L, Shi C, Xia X D. Research progress on antimicrobial effects and application of pomegranate peel extract. Food & Machinery, 2021; 37(2): 215–219. (in Chinese)

[7] Zhang J, Ma B, Wang M, Wang H, Gao Y J. Design and research of pomegranate threshing machine. The Journal of New Industrialization, 2019; 9(12): 64–67. (in Chinese)

[8] Wang M, Zhang Y O, Liu K Y, Dong X H, Wang X, Yin J C. Parameter optimization and test of vibration type pomegranate threshing device. Journal of Agricultural Mechanization Research, 2022; 44(4): 188–192. (in Chinese)

[9] Fu J, Chen Z, Han L J, Ren L Q. Review of grain threshing theory and technology. Int J Agric & Biol Eng, 2018; 11(3): 12–20.

[10] Wang R X, Zhao X P, Ji J T, Jin X, Li B. Design and performance analysis of tangential-axial flow threshing device for oat harvester. Int J Agric & Biol Eng, 2021; 14(6): 61–67.

[11] Di Z F, Cui Z K, Zhang H, Zhou J, Zhang M Y, Bu L X. Design and experiment of rasp bar and nail tooth combined axial flow corn threshing cylinder. Transactions of CSAE, 2018; 34(1): 28–34. (in Chinese)

[12] Wang Z B, Wang Z W, Zhang Y P, Yan W X, Chi Y J, Liu C Q. Design and test of longitudinal axial flexible hammer-calw corn thresher. Transaction of CASE, 2020; 51(S2): 109–117. (in Chinese)

[13] Zhu X L, Chi R J, Du Y F, Qin J H, Xiong Z X, Zhang W T, et al. Experimental study on the key factors of low-loss threshing of high-moisture maize. Int J Agric & Biol Eng, 2020; 13(5): 23–31.

[14] Li X Y, Du Y F, Mao E R, Zhang Y A, Liu L, Guo D F. Design and experiment of corn low damage threshing device based on DEM. Int J Agric & Biol Eng, 2023; 16(3): 55–63.

[15] Liu Y X, Zhao W Y, Dai F, Shi R J, Zhang S L, Fu Q F. Optionmization of the working parameters and performance experiment of diameter changes and varied-line-spacing seed corn threshing model machine. Journal of Chinese Agricultural Mechanization, 2020; 41(11): 66–74. (in Chinese)

[16] Xiang S N, Fu J, Zhang Y C. Research progress of corn threshing technology and device. Journal of Chinese Agricultural Mechanization, 2019; 40(3): 95–101. (in Chinese)

[17] Dai F, Zhao Y M, Liu Y X, Shi R J, Xin S L, Fu Q F, et al. Analysis and performance test on dynamic aril corn threshing and conveying process with variable diameter and spacing. Int J Agric & Biol Eng, 2023; 16(2): 259–266.

[18] Yilmaz D, Gökduman M E. Determination of threshing and separation unit performance of rosemary plants. Int J Agric & Biol Eng, 2021; 14(6): 237–243.

[19] Song Z C, Diao P S, Chen M Z, Miao H Q, Xu G F, Wang J X. Analysis design and test of longitudinal flow corn threshing and separating plant. Agricultural Mechanization Research, 2022; 44(2): 58–66. (in Chinese)

[20] Wang S S, Lyu W Z, Jin X, Yu S, Guo H, Chen Z H. Calibration of discrete element simulation parameters and threshing test for complete wheat plants. Int J Agric & Biol Eng, 2025; 18(3): 12–18.

[21] Yang S P, Zhang Z G, Guo G, Zhang Y, Qiu S L, Ye Y X. Optimal design and test of the flexible clamping device for safflower. Int J Agric & Biol Eng, 2025; 18(3): 19–24.

[22] Denarda A R, Bertetto A M, Carbone G. Designing a low-cost mechatronic device for semi-automatic saffron harvesting. Machines, 2021; 9(5): 94.

[23] Sun H Y, Ma H Q, Zhao Y Z. DEM investigation on conveying of nonspherical particles in a screw conveyor. Particuology, 2022; 65: 17–31.

[24] Zhu Z S, Zhang J X, Yang L L, Mao W L, Wang Y C. Design of apricot core-breaking device with squeeze-tooth-to-roller and analysis of the strength of pressing roller. Food and Machinery, 2021; 37(5): 115–119, 202. (in Chinese)

[25] He Y C, Wang X J, Cao S L, Wang M, Liu H T. Design and experimental research on twin-roll crushing device for walnut shelling. Jiangsu Agricultural Science, 2012; 40(9): 350–352. (in Chinese)